

Adiabatic-to-nonadiabatic crossover observed in the electron waiting times of a dynamically driven single-electron transistor

Fredrik Brange,¹ Adrian Schmidt,² Johannes C. Bayer,² Timo Wagner,² Christian Flindt,¹ and Rolf J. Haug²

¹*Department of Applied Physics, Aalto University, 00076 Aalto, Finland*

²*Institut für Festkörperphysik, Leibniz Universität Hannover, Hannover, Germany*

(Dated: June 14, 2022)

arXiv:2005.06176v1 [cond-mat.mes-hall] 13 May 2020

The response of a physical system to an external driving force is essential across a wide range of sciences and technologies.¹ For slow driving speeds, an adiabatic situation can be established in which the driven system is in sync with the external modulations.² However, with increasing driving frequency, the system may start to lag behind the external force as nonadiabatic processes begin to dominate. Understanding the interplay between response times and driving frequencies is of critical importance for applications that require carefully timed operations such as interferometric experiments^{3–8} and metrological current standards.^{9–11} Here, we observe an adiabatic-to-nonadiabatic crossover in a dynamically driven single-electron transistor by measuring the waiting times between emitted electrons.^{12–17} Our highly accurate experiment allows us to investigate the gradual transition from adiabatic to nonadiabatic dynamics by measuring temporal fluctuations at the single-electron level, which are captured by theory^{14,16} that covers all driving frequencies. Our work demonstrates that waiting time distributions are important for the analysis of dynamic processes in the time domain,^{14–17} and it paves the way for future technologies that rely on the ability to control, transmit, and detect single quanta of charge² or heat¹⁸ in the form of electrons,^{3–11} photons,¹⁹ or phonons.²⁰

The waiting time that passes between consecutive physical events is an important concept in the analysis of stochastic processes^{13,21} in molecular chemistry,²² quantum optics,²³ and electron transport.¹² Measuring the full distribution of waiting times, however, is challenging, since it requires nearly perfect detectors and high statistical accuracy. Still, experiments on waiting time distributions^{24–26} are motivated, for instance, by the prospects of analyzing dynamic processes in the time domain.^{14–17} Figure 1a shows our nanoscale single-electron transistor consisting of a quantum dot coupled to external electrodes defined by electrostatic gating of a two-dimensional electron gas. The system is operated in the Coulomb blockade regime, where the quantum dot can be occupied by only zero or one electron at a time. A small voltage, $V_{SD} = 1$ mV, drives a current run through the quantum dot. In addition, we apply a harmonic drive to the gate electrodes, $V_G(t) = \Delta V \sin(2\pi ft)$, with amplitude $\Delta V = 30$ mV and adjustable frequency f in the kilohertz range. The gate voltage modulates the tun-

neling of electrons in and out of the quantum dot with rates that to a good approximation depend exponentially on the external driving as $\Gamma_i(t) = \Gamma_i \exp[\alpha_i \sin(2\pi ft)]$ and $\Gamma_o(t) = \Gamma_o \exp[-\alpha_o \sin(2\pi ft)]$, where $\alpha_o = 0.85$, $\alpha_i = 0.6$, $\Gamma_o = 1.8$ kHz, and $\Gamma_i \sim 2$ kHz is weakly frequency-dependent (see Methods). To detect the individual tunneling events, we measure a separate electrical current that runs through a capacitively coupled quantum point contact, whose conductance depends sensitively on the occupation of the quantum dot.

Figure 1b shows a typical time-trace of the current in the quantum point contact, illustrating how it switches between two distinct levels in real-time, signaling that single electrons tunnel in and out of the quantum dot. To analyze the response of the system to the external drive, we measure the waiting times between electrons tunneling out of the quantum dot, τ , and their statistical distribution, $\mathcal{W}(\tau)$. Figure 1c shows the distribution of waiting times collected from about 10^6 detected tunneling events during a measurement time of approximately 10 minutes and a driving frequency of $f = 0.25$ kHz. The waiting time distribution is suppressed to zero at short times, since the quantum dot cannot be doubly occupied, and the strong Coulomb interactions thereby prevent two electrons from leaving the quantum dot simultaneously. At later times, the quantum dot can be refilled, and the suppression is gradually lifted with the distribution peaking at around $\tau \simeq 0.6$ ms, before it vanishes at much longer times. This behavior is very different from a Poisson process, such as the decay of radioactive nuclei at rate Γ , for which the distribution of waiting times is exponential, $\mathcal{W}(\tau) = \Gamma e^{-\Gamma\tau}$. Indeed, with constant rates, $\Gamma_i(t) = \Gamma_i$ and $\Gamma_o(t) = \Gamma_o$, the distribution would read¹²

$$\mathcal{W}_s(\tau, \Gamma_i, \Gamma_o) = \frac{\Gamma_i \Gamma_o}{\Gamma_i - \Gamma_o} (e^{-\Gamma_o \tau} - e^{-\Gamma_i \tau}) \quad (1)$$

with $\mathcal{W}_s(\tau, \Gamma, \Gamma) = \Gamma^2 \tau e^{-\Gamma\tau}$ for equal tunneling rates. In the experiment, the rates are time-dependent, but in Fig. 1c the driving frequency is much lower than the typical tunneling rates, $f \ll \Gamma_i, \Gamma_o$, and we expect that the system will adiabatically follow the external modulations. In that case, the waiting time distribution should be given by a period-average over the static distribution (1) with the time-dependent rates $\Gamma_i(t)$ and $\Gamma_o(t)$ inserted,¹⁶

$$\mathcal{W}(\tau) = \int_0^T \frac{dt}{T} \mathcal{W}_s(\tau, \Gamma_i(t), \Gamma_o(t)), \quad (2)$$

where $T = 1/f$ is the period of the drive. This adiabatic approximation agrees very well with the measurements,

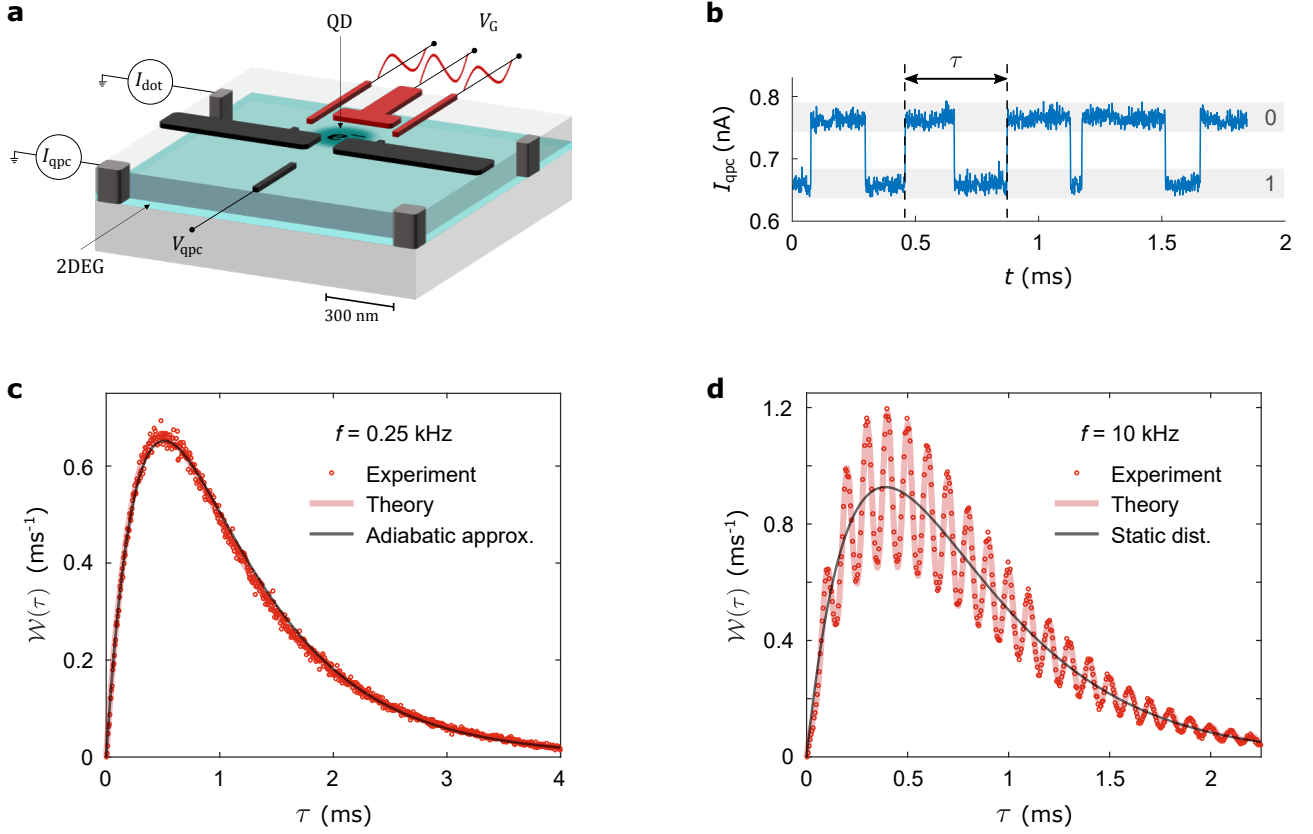


FIG. 1. **Dynamically driven single-electron transistor and waiting time distributions.** **a**, Schematic of the gate-defined quantum dot in a two-dimensional electron gas (2DEG) tunnel-coupled to two external electrodes. A harmonic voltage is applied to the gate electrodes in red, which modulates the tunneling of single electrons between the quantum dot and the leads. A capacitively coupled quantum point contact is used to monitor the charge state of the quantum dot. **b**, Time-trace of the current in the quantum point contact, which switches between two distinct levels corresponding to having 0 or 1 electron on the quantum dot. The waiting time between electrons tunneling out of the quantum dot is denoted by τ . **c**, Distribution of waiting times measured at the driving frequency $f = 0.25$ kHz together with exact calculations and the adiabatic approximation (2). **d**, Distribution measured at the driving frequency $f = 10$ kHz together with exact calculations and the static expression (1) with period-averaged rates inserted.

and it demonstrates that the system is in sync with the external drive, and the dynamic response is adiabatic.

In Fig. 1d, we have increased the driving frequency to $f = 10$ kHz, and a completely different picture now emerges. The driving frequency is much faster than the tunneling rates, and the system can no longer follow the fast high-frequency modulations. One might expect that the waiting time distribution would be given by the static result (1) with period-averaged rates, $\bar{\Gamma}_{i,o} = \int_0^T dt \Gamma_{i,o}(t)/T$, inserted. Indeed, the overall curve follows this result as shown with a black line in Fig. 1d. However, the distribution exhibits an oscillatory pattern on top of the static result, and a detailed theoretical analysis of the high-frequency regime yields the expression²⁸

$$\mathcal{W}(\tau) = \mathcal{W}_s(\tau, \bar{\Gamma}_i, \bar{\Gamma}_o) \left(1 + \frac{\alpha_o^2}{2} \cos(2\pi f \tau) \right), \quad (3)$$

which is valid up to second order in α_i and α_o . Although higher-order corrections are needed to fully capture the

experimental results, this expression explains the oscillations in the waiting time distribution with peaks occurring at multiples of the period as seen in the figure,

$$\tau_n = nT = n/f, \quad n = 1, 2, 3, \dots, \quad (4)$$

indicating that the driving is now highly nonadiabatic. In Fig. 1, we also show exact calculations²⁸ (with no adjustable parameters) that are in excellent agreement with the measurements and thus support our interpretations.

To investigate the crossover from the adiabatic to the nonadiabatic regime, waiting time distributions across the full range of driving frequencies are displayed in Fig. 2. The left panel shows experimental results for a wide range of driving frequencies, while the right panel contains the corresponding calculations of the waiting time distributions. The figure clearly illustrates how the oscillatory pattern in the waiting time distributions builds up with increasing driving frequency, and it corroborates the physical picture that peaks should appear at multiples of the driving period according to Eq. (4).

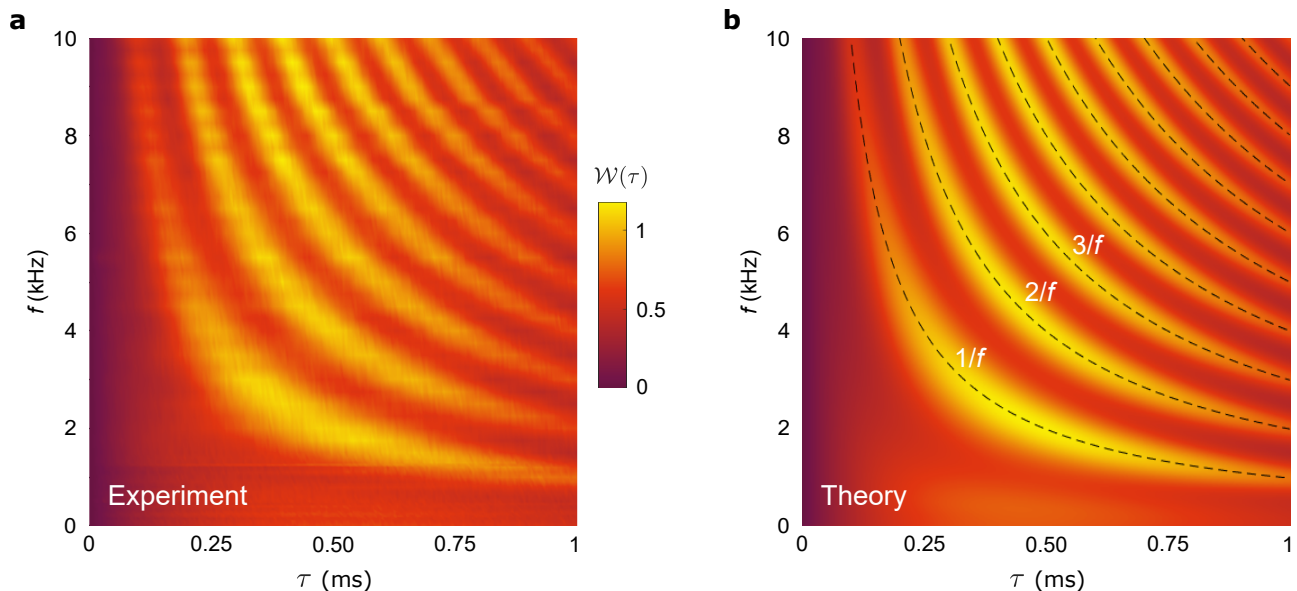


FIG. 2. **Distributions of waiting times as functions of the driving frequency.** **a**, Measured waiting time distributions with varying driving frequency f . **b**, Calculations of waiting time distributions with the parameters $\alpha_o = 0.85$, $\alpha_i = 0.6$, $\Gamma_o = 1.8$ kHz, and $\Gamma_i = 2.3$ kHz. The dashed lines indicate the peaks in the distributions at $\tau_n = n/f$ according to Eq. (4).

From our theoretical analysis, we anticipate that the crossover from adiabatic to nonadiabatic dynamics will take place for driving frequencies that are on the order of the tunneling rates; a regime, where a stochastic resonance occurs.²⁷ To explore the crossover in further detail, Fig. 3 displays distributions in this frequency range.

The leftmost panel of Fig. 3 shows the waiting time distribution for $f = 0.5$ kHz. Here, the distribution is still dominated by the adiabatic peak at short waiting times, however, a small shoulder developing at the period of the drive provides the first indications of a nonadiabatic response. In the next panel, the frequency has been increased to $f = 0.7$ kHz, and a peak is now becoming visible at the period of the drive together with a shoulder at twice the period. In the third panel, we have further increased the frequency to $f = 1$ kHz, and the waiting time distribution is now distinctly dominated by peaks at multiples of the period, signaling that we are reaching the nonadiabatic regime. Finally, in the rightmost panel with $f = 2$ kHz, the waiting time distribution is completely governed by the nonadiabatic peak structure, and we no longer see traces of the adiabatic distribution.

Our work establishes waiting times as an important experimental concept in the time-domain analysis of dynamic processes,^{12–17} here with emphasis on the adiabatic-to-nonadiabatic crossover in a driven single-electron transistor. While the present work concerns tunneling of confined electrons in a low-dimensional structure, future experiments may measure the waiting times between charge pulses propagating in extended electronic wave guides.^{3–7} These efforts are important for future quantum technologies that require carefully timed operations, such as interferometric experiments

and sensors,^{3–8} and metrological current standards based on regular single-electron emitters.^{9–11} Experiments on waiting time distributions are interesting for a wide range of physical systems, not only with electrons, but also involving other discrete quanta, for instance, single photons¹⁹ or phonons.²⁰

Methods

Experimental details. The device is based on a GaAs/AlGaAs heterostructure with a two-dimensional electron gas (2DEG). The 2DEG is formed 100 nm below the surface of the heterostructure and has a charge density of $2.4 \cdot 10^{11} \text{ cm}^{-2}$ with a mobility of $5 \cdot 10^5 \text{ cm}^2 \text{ V}^{-1} \text{ s}^{-1}$. On the surface of the heterostructure, CrAu gates are formed by e-beam and optical lithography. By applying negative gate voltages, the 2DEG below the gates is depleted and the quantum dot as well as the quantum point contact are formed.

The device was operated in a ^4He cryostat at 1.5 K, while the signal processing was done outside at room temperature. The driving signal was generated with the help of an Adwin Pro2 real-time system. To amplify the current through the quantum point contact, a low-noise amplifier with 100 kHz bandwidth was used. The detector current $I_{\text{qpc}}(t)$ was monitored with a temporal resolution of $\Delta t_s = 2.5 \mu\text{s}$. To extract the waiting times, the time-dependent occupation of the quantum dot was determined. To this end, the measured traces of $I_{\text{qpc}}(t)$ were digitized with the high current level indicating that the quantum dot was empty (state 0) and the low current level that it was occupied (state 1). The waiting times, τ , between single electrons tunneling out of the quantum dot were identified as the time between

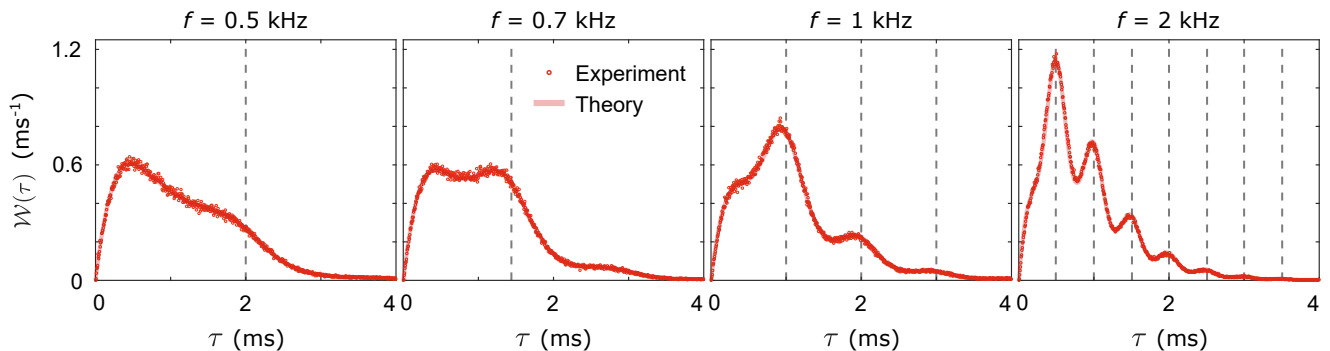


FIG. 3. **Adiabatic-to-nonadiabatic crossover.** Distributions of electron waiting times for four driving frequencies in the crossover region, $f = 0.5$ kHz (left), 0.7 kHz, 1 kHz, and 2 kHz (right). Vertical dashed lines indicate multiples of the period.

consecutive transitions from state 1 to state 0. The time-dependent tunneling rates $\Gamma_i(t)$ and $\Gamma_o(t)$ were extracted from the experimental data, and the parameters α_o , α_i , Γ_o and Γ_i were subsequently determined. We found that the first three parameters were constant, while Γ_i was weakly frequency-dependent as illustrated in the table:

f (kHz)	0.00	0.25	0.50	0.70	1.00	2.00	4.00	8.00	10.0
Γ_i (kHz)	1.80	1.95	1.70	1.70	1.60	2.30	2.20	2.55	2.80

Theory. The system can be described by the rate equation $\frac{d}{dt}|p(t)\rangle = \mathbf{L}(t)|p(t)\rangle = [\mathbf{L}_0(t) + \mathbf{J}(t)]|p(t)\rangle$, where the vector $|p(t)\rangle = (p_0(t), p_1(t))^T$ contains the probabilities for the quantum dot to be empty or occupied, and we have partitioned the rate matrix $\mathbf{L}(t)$ into

$$\mathbf{L}_0(t) = \begin{pmatrix} -\Gamma_i(t) & 0 \\ \Gamma_i(t) & -\Gamma_o(t) \end{pmatrix} \text{ and } \mathbf{J}(t) = \begin{pmatrix} 0 & \Gamma_o(t) \\ 0 & 0 \end{pmatrix},$$

where $\Gamma_{i,o}(t)$ are the tunneling rates, and $\mathbf{J}(t)$ describes electrons tunneling out of the quantum dot. The waiting time distribution can be calculated as $\mathcal{W}(\tau) = \langle \tau \rangle \partial_\tau^2 \Pi(\tau)$, where $\langle \tau \rangle = -1/[\partial_\tau \Pi(0)]$ is the mean waiting time, and $\Pi(\tau)$ is the idle-time probability that no electrons have tunneled out of the quantum dot during a time span of duration τ .^{15,16} For a periodically-driven system, this probability depends not only on the length of the interval, τ , but also on the starting point, t_0 , and we have to average it over a period of the drive as $\Pi(\tau) = \int_0^T dt_0 \Pi(\tau, t_0)/T$. The idle-time probability can

be expressed as $\Pi(\tau, t_0) = \langle 1 | \hat{T} \{ e^{\int_{t_0}^{\tau+t_0} dt \mathbf{L}_0(t)} \} | p_s(t_0) \rangle$, where \hat{T} is the time-ordering operator, the periodic state is denoted as $|p_s(t_0)\rangle = |p_s(t_0 + T)\rangle$, and we have defined $\langle 1 | = (1, 1)$.¹⁶ The periodic state is found by solving the eigenproblem, $\hat{T} \{ e^{\int_{t_0}^{\tau+t_0} dt \mathbf{L}_0(t)} \} |p_s(t_0)\rangle = |p_s(t_0)\rangle$, for $|p_s(t_0)\rangle$ by using the normalization, $p_0(t_0) + p_1(t_0) = 1$, at all times.

Acknowledgements

The work was financially supported by Deutsche Forschungsgemeinschaft (DFG, German Research Foundation) under Germany's Excellence Strategy – EXC 2123/1, the State of Lower Saxony, Germany, via Hannover School for Nanotechnology and School for Contacts in Nanosystems, and by the Academy of Finland (projects No. 308515 and 312299). F.B. acknowledges support from the European Union's Horizon 2020 research and innovation programme under the Marie Skłodowska–Curie grant agreement No. 892956.

Author contributions

T.W. carried out the experiment and A.S. processed the measurement data with support from J.C.B. The theory was developed by F.B. and C.F. All authors participated in the discussions of the results. The manuscript was prepared by F.B., C.F., A.S., and R.J.H. The research was supervised by C.F. and R.J.H.

Competing interests

The authors declare no competing interests.

¹ A. Pikovsky, J. Kurths, and M. Rosenblum, *Synchronization: A Universal Concept in Nonlinear Sciences* (Cambridge University Press, 2001).

² J. Splettstoesser and R. J. Haug, “Special issue on single-electron control in solid state devices,” *Phys. Status Solidi B* **254**, 1770217 (2017).

³ G. Fève, A. Mahé, J.-M. Berroir, T. Kontos, B. Plaçaïs, D. C. Glatli, A. Cavanna, B. Etienne, and Y. Jin,

“An On-Demand Coherent Single-Electron Source,” *Science* **316**, 1169 (2007).

⁴ E. Bocquillon, V. Freulon, J.-M. Berroir, P. Degiovanni, B. Plaçaïs, A. Cavanna, Y. Jin, and G. Fève, “Coherence and Indistinguishability of Single Electrons Emitted by Independent Sources,” *Science* **339**, 1054 (2013).

⁵ E. Bocquillon, V. Freulon, F. D. Parmentier, J.-M. Berroir, B. Plaçaïs, C. Wahl, J. Rech, T. Jonckheere, T. Martin,

- C. Grenier, D. Ferraro, P. Degiovanni, and G. Fve, “Electron quantum optics in ballistic chiral conductors,” *Ann. Phys.* **526**, 1 (2014).
- ⁶ J. Dubois, T. Jullien, P. Portier, F. and Roche, A. Cavanna, Y. Jin, W. Wegscheider, P. Roulleau, and D. C. Glattli, “Minimal-excitation states for electron quantum optics using levitons,” *Nature* **502**, 659 (2013).
- ⁷ T. Jullien, P. Roulleau, B. Roche, A. Cavanna, Y. Jin, and D. C. Glattli, “Quantum tomography of an electron,” *Nature* **514**, 603 (2014).
- ⁸ N. Ubbelohde, F. Hohls, V. Kashcheyevs, T. Wagner, L. Fricke, B. Kästner, K. Pierz, H. W. Schumacher, and R. J. Haug, “Partitioning of on-demand electron pairs,” *Nat. Nanotech.* **10**, 46 (2014).
- ⁹ M. D. Blumenthal, B. Kaestner, L. Li, S. Giblin, T. J. B. M. Janssen, M. Pepper, D. Anderson, G. Jones, and D. A. Ritchie, “Gigahertz quantized charge pumping,” *Nat. Phys.* **3**, 343 (2007).
- ¹⁰ J. P. Pekola, O.-P. Saira, V. F. Maisi, A. Kemppinen, M. Möttönen, Yu. A. Pashkin, and D. V. Averin, “Single-electron current sources: Toward a refined definition of the ampere,” *Rev. Mod. Phys.* **85**, 1421 (2013).
- ¹¹ B. Kaestner and V. Kashcheyevs, “Non-adiabatic quantized charge pumping with tunable-barrier quantum dots: a review of current progress,” *Rep. Prog. Phys.* **78**, 103901 (2015).
- ¹² T. Brandes, “Waiting times and noise in single particle transport,” *Ann. Phys.* **17**, 477 (2008).
- ¹³ S. L. Rudge and D. S. Kosov, “Counting quantum jumps: A summary and comparison of fixed-time and fluctuating-time statistics in electron transport.” *J. Chem. Phys.* **151**, 034107 (2019).
- ¹⁴ M. Albert, C. Flindt, and M. Büttiker, “Distributions of Waiting Times of Dynamic Single-Electron Emitters,” *Phys. Rev. Lett.* **107**, 086805 (2011).
- ¹⁵ D. Dasenbrook, C. Flindt, and M. Büttiker, “Floquet Theory of Electron Waiting Times in Quantum-Coherent Conductors,” *Phys. Rev. Lett.* **112**, 146801 (2014).
- ¹⁶ E. Potanina and C. Flindt, “Electron waiting times of a periodically driven single-electron turnstile,” *Phys. Rev. B* **96**, 045420 (2017).
- ¹⁷ P. Buset, J. Kotilahti, M. Moskalets, and C. Flindt, “Time-Domain Spectroscopy of Mesoscopic Conductors Using Voltage Pulses,” *Adv. Quant. Technol.* **2**, 1900014 (2019).
- ¹⁸ J. P. Pekola, “Towards quantum thermodynamics in electronic circuits,” *Nat. Phys.* **11**, 118 (2015).
- ¹⁹ I. Aharonovich, D. Englund, and M. Toth, “Solid-state single-photon emitters,” *Nat. Photon.* **10**, 631 (2016).
- ²⁰ J. D. Cohen, S. M. Meenehan, G. S. MacCabe, S. Gröblacher, A. H. Safavi-Naeini, F. Marsili, M. D. Shaw, and O. Painter, “Phonon counting and intensity interferometry of a nanomechanical resonator,” *Nature* **520**, 522 (2015).
- ²¹ N. G. Van Kampen, *Stochastic Processes in Physics and Chemistry* (North Holland, 2007).
- ²² B. P. English, W. Min, A. M. van Oijen, K. T. Lee, G. Luo, H. Sun, B. J. Cherayil, S. C. Kou, and X. S. Xie, “Ever-fluctuating single enzyme molecules: Michaelis-Menten equation revisited,” *Nat. Chem. Biol.* **2**, 87 (2006).
- ²³ H. J. Carmichael, S. Singh, R. Vyas, and P. R. Rice, “Photoelectron waiting times and atomic state reduction in resonance fluorescence,” *Phys. Rev. A* **39**, 1200 (1989).
- ²⁴ A. Delteil, W.-b. Gao, P. Fallahi, J. Miguel-Sanchez, and A. Imamoglu, “Observation of Quantum Jumps of a Single Quantum Dot Spin Using Submicrosecond Single-Shot Optical Readout,” *Phys. Rev. Lett.* **112**, 116802 (2014).
- ²⁵ S. K. Gorman, Y. He, M. G. House, J. G. Keizer, D. Keith, L. Fricke, S. J. Hile, M. A. Broome, and M. Y. Simmons, “Tunneling statistics for analysis of spin-readout fidelity,” *Phys. Rev. Applied* **8**, 034019 (2017).
- ²⁶ M. Jenei, E. Potanina, R. Zhao, K. Y. Tan, A. Rossi, T. Tantt, K. W. Chan, V. Sevriuk, M. Möttönen, and A. Dzurak, “Waiting time distributions in a two-level fluctuator coupled to a superconducting charge detector,” *Phys. Rev. Research* **1**, 033163 (2019).
- ²⁷ T. Wagner, P. Talkner, J. C. Bayer, E. P. Rugeramigabo, P. Hänggi, and R. J. Haug, “Quantum stochastic resonance in an a.c.-driven single-electron quantum dot,” *Nat. Phys.* **15**, 330 (2019).
- ²⁸ See supplementary information.

Supplementary information:

Adiabatic-to-nonadiabatic crossover observed in the electron waiting times of a dynamically driven single-electron transistor

Fredrik Brange,¹ Adrian Schmidt,² Johannes C. Bayer,² Timo Wagner,² Christian Flindt,¹ and Rolf J. Haug²

¹*Department of Applied Physics, Aalto University, 00076 Aalto, Finland*

²*Institut für Festkörperphysik, Leibniz Universität Hannover, Hannover, Germany*

CALCULATIONS OF WAITING TIME DISTRIBUTIONS

A. Numerical calculations

To calculate the distribution of waiting times we follow Ref. 1 and the Methods section. We first compute the idle-time probability as $\Pi(\tau, t_0) = \langle 1 | \mathbf{U}_0(\tau + t_0, t_0) | p_s(t_0) \rangle$ with $\mathbf{U}_0(t, t_0) = \hat{T} \{ e^{\int_{t_0}^t dt_1 \mathbf{L}_0(t_1)} \}$, where \hat{T} is the time-ordering operator and $\langle 1 | \equiv (1, 1)$. For the periodic state, $| p_s(t_0) \rangle = | p_s(t_0 + T) \rangle$, we find

$$p_0(t_0) = \frac{e^{-\int_{t_0}^{t_0+T} dt_1 (\Gamma_i(t_1) + \Gamma_o(t_1))}}{1 - e^{-\int_{t_0}^{t_0+T} dt_1 (\Gamma_i(t_1) + \Gamma_o(t_1))}} \int_{t_0}^{t_0+T} dt_1 \Gamma_i(t_1) e^{\int_{t_0}^{t_1} dt_2 [\Gamma_i(t_2) + \Gamma_o(t_2)]}. \quad (1)$$

with the normalization, $p_0(t_0) + p_1(t_0) = 1$, at all times. For the non-zero matrix elements of $\mathbf{U}_0(t, t_0)$, we have [1]

$$\begin{aligned} [\mathbf{U}_0(t, t_0)]_{11} &= \exp \left[- \int_{t_0}^t dt_1 \Gamma_i(t_1) \right], & [\mathbf{U}_0(t, t_0)]_{22} &= \exp \left[- \int_{t_0}^t dt_1 \Gamma_o(t_1) \right], \\ [\mathbf{U}_0(t, t_0)]_{21} &= \exp \left[- \int_{t_0}^t dt_1 \Gamma_o(t_1) \right] \int_{t_0}^t dt_1 \Gamma_i(t_1) \exp \left[\int_{t_0}^{t_1} dt_2 [\Gamma_o(t_2) - \Gamma_i(t_2)] \right], \end{aligned} \quad (2)$$

and thereby obtain

$$\Pi(\tau, t_0) = U_{11}(t_0 + \tau, t_0)[1 - p_0(t_0)] + U_{21}(t_0 + \tau, t_0)[1 - p_0(t_0)] + U_{22}(t_0 + \tau, t_0)p_0(t_0). \quad (3)$$

By evaluating these expressions numerically, we obtain the waiting time distribution as $\mathcal{W}(\tau) = \langle \tau \rangle \partial_\tau^2 \Pi(\tau)$ with $\langle \tau \rangle = -1/[\partial_\tau \Pi(\tau = 0)]$ and $\Pi(\tau) = \int_0^T dt_0 \Pi(\tau, t_0)/T$.

B. Zero-frequency limit

With constant rates, $\Gamma_i(t) = \Gamma_i$ and $\Gamma_o(t) = \Gamma_o$, Eqs. (1) and (2) are easily solved analytically, yielding

$$p_0^s(t_0, \Gamma_i, \Gamma_o) = \frac{\Gamma_i}{\Gamma_i + \Gamma_o}, \quad (4)$$

and

$$\begin{aligned} [\mathbf{U}_0(t, t_0, \Gamma_i)]_{11}^s &= \exp[-\Gamma_i(t - t_0)], & [\mathbf{U}_0(t, t_0, \Gamma_o)]_{22}^s &= \exp[-\Gamma_o(t - t_0)], \\ [\mathbf{U}_0(t, t_0, \Gamma_i, \Gamma_o)]_{21}^s &= \frac{\Gamma_i}{\Gamma_i - \Gamma_o} \left(e^{-\Gamma_o(t-t_0)} - e^{-\Gamma_i(t-t_0)} \right). \end{aligned} \quad (5)$$

We then find

$$\Pi_s(t, \Gamma_i, \Gamma_o) = \frac{e^{-\Gamma_o t} \Gamma_i^2 - e^{-\Gamma_i t} \Gamma_o^2}{\Gamma_i^2 - \Gamma_o^2}, \quad (6)$$

and

$$\mathcal{W}_s(\tau, \Gamma_i, \Gamma_o) = \frac{\Gamma_i \Gamma_o}{\Gamma_i - \Gamma_o} \left(e^{-\Gamma_o \tau} - e^{-\Gamma_i \tau} \right), \quad (7)$$

which is Eq. (1) of the main text.

C. High-frequency limit

For $\alpha_i, \alpha_o \ll 1$, we may treat the driving as a perturbation and expand all quantities to second order in the driving amplitudes (the first-order contribution to the waiting time distribution eventually vanishes). We start by expanding the tunneling rates as

$$\Gamma_i(t) = \Gamma_i \left[1 + \alpha_i \sin(2\pi ft) + \frac{1}{2} \alpha_i^2 \sin^2(2\pi ft) \right], \quad \Gamma_o(t) = \Gamma_o \left[1 - \alpha_o \sin(2\pi ft) + \frac{1}{2} \alpha_o^2 \sin^2(2\pi ft) \right]. \quad (8)$$

We note that the average values of the rates over a full driving period are

$$\bar{\Gamma}_i = \frac{1}{T} \int_0^T dt \Gamma_i(t) = \Gamma_i(1 + \alpha_i^2/4), \quad \bar{\Gamma}_o = \frac{1}{T} \int_0^T dt \Gamma_o(t) = \Gamma_o(1 + \alpha_o^2/4). \quad (9)$$

In principle, second-order perturbation theory allows us to derive an analytic expression for the waiting time distribution for all frequencies. However, given the lengthy expressions that the general derivation yields, we focus here on the high-frequency limit, $f \gg \Gamma_i, \Gamma_o$, where all expressions may be simplified considerably. Below we expand each quantity around its corresponding steady-state equivalent with the averaged rates $\bar{\Gamma}_i$ and $\bar{\Gamma}_o$ inserted. We neglect terms that are negligible in the high-frequency limit, $f \gg \Gamma_i, \Gamma_o$ and then find

$$p_0(t_0) = p_0^s(t_0, \bar{\Gamma}_i, \bar{\Gamma}_o) \left(1 - \frac{\Gamma_o}{2\pi f} \cos(2\pi ft_0) (\alpha_i + \alpha_o) \right), \quad (10)$$

as well as

$$[\mathbf{U}_0(t, t_0)]_{11} = [\mathbf{U}_0(t, t_0, \bar{\Gamma}_i)]_{11}^s (1 + \gamma_i + \gamma_i^2/2), \quad [\mathbf{U}_0(t, t_0)]_{22} = [\mathbf{U}_0(t, t_0, \bar{\Gamma}_o)]_{22}^s (1 + \gamma_o + \gamma_o^2/2), \quad (11)$$

and

$$\begin{aligned} [\mathbf{U}_0(t, t_0)]_{21} = & [\mathbf{U}_0(t, t_0, \bar{\Gamma}_i, \bar{\Gamma}_o)]_{21}^s \left(1 + \frac{\cos[2\pi ft]}{2\pi f} \left[\frac{e^{\Gamma_o t + \Gamma_i t_0} \alpha_i (\Gamma_i - \Gamma_o)}{e^{\Gamma_o t + \Gamma_i t_0} - e^{\Gamma_i t + \Gamma_o t_0}} - \alpha_o \Gamma_o \right] + \frac{1}{2(2\pi f)^2} \left[\alpha_i \alpha_o \Gamma_i \Gamma_o \cos(2\pi f(t - t_0)) \right. \right. \\ & \left. \left. - \frac{2\alpha_i (\Gamma_i - \Gamma_o) (e^{\Gamma_o t + \Gamma_i t_0} \cos(2\pi ft) - e^{\Gamma_i t + \Gamma_o t_0} \cos(2\pi ft_0)) (\alpha_o \Gamma_o \cos(2\pi ft) + \alpha_i \Gamma_i \cos(2\pi ft_0))}{e^{\Gamma_o t + \Gamma_i t_0} - e^{\Gamma_i t + \Gamma_o t_0}} \right] \right), \end{aligned} \quad (12)$$

with $\gamma_x \equiv \frac{\alpha_x \Gamma_x}{2\pi f} (\cos[2\pi ft] - \cos[2\pi ft_0])$, $x = i, o$. In the expressions above for the matrix elements of $\mathbf{U}_0(t, t_0)$, we have omitted terms that eventually vanish when averaged over a period of the drive. By averaging the idle-time probability in Eq. (3) over a period of the drive, we find

$$\Pi(t) = \Pi_s(t, \bar{\Gamma}_i, \bar{\Gamma}_o) \left(1 - \frac{1}{2} \left(\frac{1}{2\pi f} \right)^2 \frac{\Gamma_i^2 \Gamma_o^2 (e^{\Gamma_i t} - e^{\Gamma_o t})}{e^{\Gamma_i t} \Gamma_i^2 - e^{\Gamma_o t} \Gamma_o^2} \cos(2\pi ft) \alpha_o^2 \right), \quad (13)$$

and we then arrive at the high-frequency expression for the waiting time distribution in Eq. (3) of the main text,

$$\mathcal{W}(\tau) = \mathcal{W}_s(\tau, \bar{\Gamma}_i, \bar{\Gamma}_o) \left[1 + \frac{\alpha_o^2}{2} \cos(2\pi f\tau) \right]. \quad (14)$$

[1] E. Potanina and C. Flindt, “Electron waiting times of a periodically driven single-electron turnstile,” *Phys. Rev. B* **96**, 045420 (2017).